2010
2011

FACULTY OF SCIENCES

Master of Statistics: Biostatistics

Masterproef

Effect of cooling post-cardiac arrest patients

Promotor :
dr. Herbert THIJS
De heer Edmund NJAGI

Promotor :
Dr. JO DENS
Drs. INGRID MEEX

Kimeu Muthusi

Master Thesis nominated to obtain the degree of Master of Statistics , specialization Biostatistics

De transnationale Universiteit Limburg is een uniek samenwerkingsverband van twee universiteiten in twee landen: de Universiteit Hasselt en Maastricht University

universiteit hasselt
UNIVERSITEIT VAN DE TOEKOMST

Maastricht University

Universiteit Hasselt | Campus Diepenbeek | Agoralaan Gebouw D | BE-3590 Diepenbeek
Universiteit Hasselt | Campus Hasselt | Martelarenlaan 42 | BE-3500 Hasselt

Maastricht University

universiteit hasselt
UNIVERSITEIT VAN DE TOEKOMST

2010
2011

FACULTY OF SCIENCES

Master of Statistics: Biostatistics

Masterproef

Effect of cooling post-cardiac arrest patients

Promotor :
dr. Herbert THIJS
De heer Edmund NJAGI

Promotor :
Dr. JO DENS
Drs. INGRID MEEX

Kimeu Muthusi

Master Thesis nominated to obtain the degree of Master of Statistics , specialization Biostatistics

Maastricht University

universiteit hasselt
UNIVERSITEIT VAN DE TOEKOMST

Acknowledgements

Foremost, I would like to appreciate Jo Dens and the team of researchers at Ziekenhuis Oost-Limburg, Genk for offering me the summer internship opportunity and providing data and research questions for this project. I wish to thank specially Ingrid Meex, PhD student, Department of Morphology, University of Hasselt, for providing clinical explanations and clarifications to issues surrounding the data and the study in general.

I wish thank to Herbert Thijs, of I-BioStat, University of Hasselt, for providing advice and guidelines on statistical methods used during data analysis. I also acknowledge Edmund Njagi, PhD student, CenStat, University of Hasselt, for stimulating discussions and material support during data analysis.

I am deeply grateful to the Flemish Interuniversity Council (VLIR) for offering me scholarship to pursue this valuable Masters program. I acknowledge my fellow students and lecturers for providing an intellectually stimulating environment during the program. I also acknowledge Martine Machiels and other staff at the secretariat for their continued support throughout the program.

Last but not least, I am grateful to my wife Jane, for her magnificent devotion to the family and her unyielding support, my son Elvis for his patience and understanding during the program, and my parents for their encouragement and spiritual support throughout my life.

Kimeu Muthusi,

University of Hasselt
September 12, 2011

Abstract

Introduction: Clinical studies involving post-cardiac arrest patients have gained popularity in the recent past. This has been enhanced by presence of therapeutic hypothermia, which is a medical treatment used to regulate a patient's body temperature with the aim of reducing risk of ischemic injury to tissues following a period of insufficient blood flow due to cardiac arrest. Cerebral oxygen saturation was measured repeatedly over time for each patient during each phase of the therapy. The study aimed to investigate trend and variability of cerebral oxygen saturation over time in each patient group as well as its correlations with other parameters.

Methods: Generalized additive models (GAM) was preferred over generalized linear models (GLM),considered as standard approach, due to complexities arising from the small sample size available. GAM also have the advantage of flexibility by using smoothing functions instead of parametric terms to estimate trend. To incorporate patient-to-patient variation, GAM was extended to generalized additive mixed models (GAMM) by inclusion of random effects.

Results: In the cooling phase, trend of cerebral oxygen saturation in survivor group started at lower values compared to non-survivor group. It then increased rapidly to reach a maximum peak before a gradual decrease to reach a minimum peak followed by a gradual increase towards baseline measurements. Trend for non-survivor group was found to start at higher values than survivor group but decreased gradually over time. Further, it was found that in the cooling phase some significant differences were evinced between patient groups in terms of trend. In other phases, no significant differences were observed.

Conclusion: Some challenges were encountered which included among other large repeated measures profiles, highly unbalanced time series, and limitations in computer memory for use by software. These led to data reduction through truncation and aggregation. Researchers were, however, urged to consider possibility of increasing sample size and/or employing other statistical methods that would overcome such challenges.

Keywords: Generalized additive models, Generalized linear models, Therapeutic hypothermia, Time series data.

Contents

List of Tables

List of Figures

1 Introduction

1.1 Methodological Background

Research in the medical field is often associated with studies designed to evaluate the evolution of a patient's characteristic of interest, mostly a disease or effect of medical procedure on patient management. In such a case, patient measurements are taken over time to determine modality of evolution of a patient characteristic, a typical feature of longitudinal settings Diggle et al. (2002). Due to the longitudinal nature of such data, classical approaches to data analysis fail due to lack of independence of observations as measurements per patient are often highly correlated.

In most cases, interest often lies in understanding the evolution of individual patient characteristics and how this evolution is influenced by a set of independent variables. This proves even to be essential when individual interventions may be necessary. Such is the case in this project where cerebral oxygen saturation for post-cardiac arrest patients enrolled in therapeutic hypothermia was studied as an indicator of patient survival. Subject specific models are useful in such cases, that is, when interest is in within-patient changes (Neuhaus et al., 1992).

To analyze such data, generalized linear models (GLM) approach, first introduced by Harville (1974), and discussed in detail by Laird and Ware (1982) is considered a standard approach (Verbeke and Molenberghs, 2000; Molenberghs and Verbeke, 2005). This approach is particularly applauded for its ability to account for heterogeneity, serial correlation, dropouts and handling of intermediate missing values. It is also useful in studies with overlapping levels of within-patient factors (e.g., patient group and time) as well as between-patient factors to study, for instance, patient group-response relationships.

Though they have nice properties, they have a disadvantage that only a limited number of non-linear models can be turned into a GLM by choice of a link function. Additionally, when the sample size is smaller than the number of parameters to be estimated, GLM are no longer identifiable, and other approaches must be considered. Semi-parametric models provide a flexible methodological framework to work with in such cases. This is because they combine the advantages of parametric and nonparametric models by allowing for inclusion of explicit parametric terms for certain predictors and smooth non-parametric terms for others (Ruppert et al., 2003).

Generalized additive model (GAM), introduced by Hastie and Tibshirani (1990), is a spe-

cific type of semi-parametric model which assumes that the mean of a dependent variable depends on an additive predictor but not necessarily linearly (Gilks et al., 1996). GAM are useful in finding predictor-response relationships in many kinds of data without using a specific model. They combine the ability to explore many non-parametric relationships simultaneously with distributional flexibility of GLM. According to Hastie and Tibshirani (1990); Xiang (2002), GAM have the advantage that they allow greater flexibility than traditional parametric modeling tools. They relax the usual parametric assumption to uncover hidden structure in the relationship between dependent and independent variables. This amounts to allowing for an alternative distribution for the underlying random variation besides the normal distribution. GAM can therefore be applied to a much wider range of data analysis problems. In particular, they are widely used for air pollution time-series studies (Dominici et al., 2002; Peng and Dominici, 2008; Schwartz et al., 1996).

This report demonstrates the application of GAM to investigate trend of cerebral oxygen saturation in post-cardiac arrest patients.

1.2 Study Description

This study was part of a project being conducted by researchers at Ziekenhuis Oost-Limburg, Genk, to investigate the effect of cooling in post-cardiac arrest patients enrolled in therapeutic hypothermia. Winslow (2009), define therapeutic hypothermia (also known as protective hypothermia) as a medical treatment that is used to regulate a patient's body temperature in order to help reduce the risk of the ischemic injury to tissues following a period of insufficient blood flow which may be due to cardiac arrest or occlusion of an artery by embolism, as occurs in the case of stroke. Therapeutic hypothermia may be induced by invasive means, in which a catheter is placed in the inferior vena cava via femoral vein, or by non-invasive means, usually involving a chilled water blanket or torso vest and leg wraps in direct contact with patient's skin. Studies have demonstrated that patients at risk for ischemic brain injuries have better outcomes if treated with therapeutic hypothermia (Holzer, 2002).

The therapy is usually divided into 4 main phases namely: cooling, hypothermia, rewarming and normothermia. The cooling (also known as induction) phase, represents the start of therapy and involves lowering a patient's body temperature to 33°C as quickly as possible. This is usually achieved by infusion of cold isotonic fluid. According to (So, 2010), caution should be exercised to avoid over-cooling, hypokalaemia, hyperglycaemia, and shivering. Further, issues surrounding changes in pharmacokinetics and haemodynamics, and susceptibility to infection should be addressed. The optimal duration of maintenance is not known but the usual practice is 12-24 hours. The second phase is hypothermia where patient's body temperature is

maintained at 33°C for 24 hours to give the brain time to recover from the period it did not have enough oxygen. The third phase is rewarming (also known as de-cooling) and involves increasing patient's body temperature to normal values of 37°C. Patients are usually rewarmed at a controlled rate of 0.3°C per hour. The final phase is normothermia where patients are no longer under control but are expected to maintain body temperature at 37°C on their own.

To investigate the effect of therapeutic hypothermia, cerebral oxygen saturation over time for each patient in each phase was recorded.

1.3 Study Objectives

The objectives of the study were to: (a) determine variability of cerebral oxygen saturation, both as an absolute value and over time in each patient group in each phase, (b) investigate trend of cerebral oxygen saturation over time in each patient group in each phase and (c) investigate correlations between oxygen saturation and other variables in each phase.

This report is structured so that Section 2 introduces the data followed by a description of exploratory and statistical methods in Section 3. Section 4 presents results of analysis which are discussed further in Section 5. Section 6 discusses challenges encountered during analysis and some concluding remarks.

2 Data

The data consisted of measurements taken from 12 post-cardiac arrest patients enrolled on therapeutic hypothermia. Patients were further classified into two groups, survivor and non-survivor groups, depending on whether or not they left the hospital alive. The response of interest was cerebral oxygen saturation (SctO2) measured repeatedly over time after every 2 seconds during a patient's stay in each phase. Covariates, also measured over time in each phase, were: Oesophagale temperature (OESOPHAGALE) measured after every minute and reflected central body temperature; Rectal temperature (RECTAL) measured approximately every hour and reflected peripheral temperature. Both rectal and oesophagale temperature were expected to be correlated; Cardiac output(CCO) which gave information regarding a patient's heart condition was measured after every one hour, but sometimes much often; Carbon dioxide (CO2) and Oxygen (pO2) content in the blood were measured every hour, and gave an idea about oxygen content in the blood. Unfortunately, two patients died during the study and therefore, no data was available for them in the rewarming and normothermia phases.

3 Methodology

Various exploratory and statistical methods were used to analyze trend and variability of cerebral oxygen saturation over time and its correlations with other variables.

3.1 Exploratory Data Analysis

Exploratory tools such as summary statistics and graphical representations of evolution over time profiles were used to gain insight into the data. These tools were also used to help in displaying possible interesting relationships within the data which could then be investigated using formal statistical models.

3.2 Generalized Additive Model (GAM)

Using the notation of Wood (2006), a GAM can be presented as:

$$g(\mu_i) = \boldsymbol{X}_i^*\boldsymbol{\theta} + f_1(x_{1i}) + f_2(x_{2i}) + f_3(x_{3i}, x_{4i}) + \ldots + \varepsilon_i \tag{3.1}$$

where $\mu_i \equiv E(Y_i)$ and $Y_i \sim$ some exponential family distribution, $\boldsymbol{X}_i^*$ is the design matrix, $\boldsymbol{\theta}$ the corresponding parameter vector, and $f_j(.)$ are smooth functions of covariates. Model (3.1) is simply an additive model if g is the identity link and the response is normally distributed.

3.2.1 Estimation of GAM

The first step towards GAM estimation is the choice of smoothing bases. Scatterplot smoothing functions, commonly referred to as smoothers, are central to GAM. According to Hastie and Tibshirani (1990), a smoother is a tool used for summarizing the trend of a response measurement as a function of independent variables. i.e.,

$$y_i \quad = \quad f(x_i) + \epsilon_i \tag{3.2}$$

A basis, chosen for each smooth function in the model, can be seen as a way of defining the space of functions for which f_j is an element (Wood, 2006). Choosing a basis amounts to choosing a basis function b_j such that the regression splines $f_j(x_j)$ can be represented as:

$$f_j(x_j) = \sum_{i=1}^{q_j} b_{ji}\beta_{ji}(x_j) \tag{3.3}$$

where x_j may be a vector quantity and β_{ji} are coefficient of the smooth, which are estimated as part of model fitting. Once bases have been selected, (3.1) reduces to a GLM problem. This can be demonstrated by writing each smooth function in the model in terms of a model

matrix $\tilde{\boldsymbol{X}}_{\boldsymbol{j}}$. Letting $\boldsymbol{f_j}$ be a vector such that $\boldsymbol{f}_{\boldsymbol{j}i} = f_j(x_{ji})$ and $\tilde{\boldsymbol{\beta}}_{\boldsymbol{j}} = [\beta_{j1}, \ldots, \beta_{jq_j}]'$, yields to $\boldsymbol{f_j} = \tilde{\boldsymbol{X}}_{\boldsymbol{j}}\tilde{\boldsymbol{\beta}}_{\boldsymbol{j}}$ where $\tilde{\boldsymbol{X}}_{\boldsymbol{j},ik} = b_{jk}(x_{ji})$. Model (3.1) is not identifiable unless each smooth function is subjected to a centering constraint. The sum (or mean) of the elements of $\boldsymbol{f_j}$ is, for instance, constrained to be equal to zero i.e., $\mathbf{1}'\tilde{\boldsymbol{X}}_{\boldsymbol{j}}\tilde{\boldsymbol{\beta}}_{\boldsymbol{j}} = \mathbf{0}$. When the smooth terms are re-parameterized in terms of $q_j - 1$ new parameters, $\boldsymbol{\beta_j}$, such that $\tilde{\boldsymbol{\beta}}_{\boldsymbol{j}} = \boldsymbol{Z}\boldsymbol{\beta_j}$ with $\boldsymbol{Z}$ being a matrix such that its $q_j - 1$ columns are orthogonal and the matrix also satisfies $\mathbf{1}'\tilde{\boldsymbol{X}}_{\boldsymbol{j}}\boldsymbol{Z} = \mathbf{0}$, a new model matrix for the jth term, $\boldsymbol{X_j} = \tilde{\boldsymbol{X}}_{\boldsymbol{j}}\boldsymbol{Z}$, is obtained such that, $\boldsymbol{f_j} = \boldsymbol{X_j}\boldsymbol{\beta_j}$ satisfies the centering constraint. Given the centered model matrices for the smooth functions, (3.1) can be written as $g(\mu_i) = \boldsymbol{X}_i\boldsymbol{\beta}$, where $\boldsymbol{X} = [\boldsymbol{X}^* : \boldsymbol{X_1} : \boldsymbol{X_2} : \ldots]$ and $\boldsymbol{\beta}' = [\boldsymbol{\theta}', \boldsymbol{\beta_1}', \boldsymbol{\beta_2}', \ldots]$ which is clearly a GLM.

It is important to note that, if the q_j are large enough such that there is a reasonable chance of accurately representing the unknown f_j's, and $\boldsymbol{\beta}$ is estimated by ordinary likelihood maximization, then there is a good chance of over-fitting. For this reason GAM are usually estimated by penalized likelihood maximization, where penalties are designed to suppress overly *wiggly* estimates of f_j terms. In fact, this is the idea behind the penalized regression approach of GAM estimation (Wood, 2006).

One useful basis in GAM estimation is the cubic regression splines (CRS). Splines have some theoretical properties, which make them a popular choice for penalized regression. This can be illustrated by considering their properties, in the context of interpolation and smoothing.

The natural cubic spline, $g(x)$ interpolating the points $\{x_i, y_i : i = 1, \ldots, n\}$ with $x_i < x_{i+1}$ is defined as a function composed of sections of cubic polynomial, one for each interval $[x_i, x_n]$ joined together so that the function is continuous in value, as well as its first and second derivatives, i.e., $g(x_i) = y_i$ and $g''(x_1) = g''(x_n) = 0$. The points at which the sections are joined are referred to as the *knots* of the spline. It has been shown that this function is not only the smoothest interpolator through any data set, but also provides interpolation that is optimal in various respects. Based on these properties, splines are deemed as capable of closely approximating any smooth function. Because of this property, they are considered intuitively appropriate in representing smooth terms in models (Wood, 2006).

When considered in the context of smoothing, it has been shown that cubic smoothing splines arise as a solution to the smoothing objective, which is mathematically expressed as the minimization of

$$\sum_{i=1}^{n}\{y_i - f(x_i)\}^2 + \lambda \int f''(x)^2 dx \tag{3.4}$$

where λ controls the trade-off between closely fitting the data and producing a smooth function. Given this mathematical result, the only challenge that remains before adopting them as ideal smoothers is that they have as many free parameters as there are data to be smoothed. Thus, computation becomes expensive in case of many covariates.

The use of penalized regression splines is then a compromise solution between retaining the good properties of splines and computational efficiency, the idea being to use a spline basis together with penalties to model the data at hand. Cubic regression splines are a subset of penalized regression smoothers. Though there are many ways of defining a cubic regression spline basis, one way, which has been credited to have directly interpretable parameters, is to have the spline parameterized at its values at the knots (Wood, 2006).

Other splines framework available include: thin plate regression splines, thin plate regression splines with shrinkage, cubic regression splines with shrinkage and P-splines. They are discussed in detail by Hastie and Tibshirani (1990); Wood (2006). CRS however have the advantage that they are computationally cheap when compared to other splines.

3.2.2 Penalized Iteratively Re-weighted Least Squares Estimation (P-IRLS)

Since a measure capturing how *wiggly* each smooth function in the model is now available, a penalized likelihood for the model can then be written. Penalties, which measure this as a quadratic form in the function coefficients, are considered. For the jth function, this may be evaluated by $\tilde{\boldsymbol{\beta}}_j^{'}\tilde{\boldsymbol{S}}_j\tilde{\boldsymbol{\beta}}_j$ where $\tilde{\boldsymbol{S}}_j$ is a penalty matrix of known coefficients. By re-parametrization through centering and re-writing the penalty in terms of the full coefficient vector $\boldsymbol{\beta}$, this can be expressed as $\boldsymbol{\beta}^{'}\boldsymbol{S}_j\boldsymbol{\beta}$ where $\boldsymbol{S}_j$ is simply $\bar{\boldsymbol{S}}_j$ padded with zeros such that $\boldsymbol{\beta}^{'}\boldsymbol{S}_j\boldsymbol{\beta} = \boldsymbol{\beta}^{'}\bar{\boldsymbol{S}}_j\boldsymbol{\beta}$ where $\bar{\boldsymbol{S}}_j = \boldsymbol{Z}^{'}\tilde{\boldsymbol{S}}_j\boldsymbol{Z}$. The penalized likelihood is therefore defined as

$$l_p(\boldsymbol{\beta}) = l(\boldsymbol{\beta}) - \frac{1}{2}\sum_j \lambda_j \boldsymbol{\beta}^{'}\boldsymbol{S}_j\boldsymbol{\beta} \tag{3.5}$$

where λ_j are smoothing parameters, which control the trade-off between model fit and smoothness. Given λ_j, l_p can be maximized for $\boldsymbol{\beta}$. However, λ_j have to be estimated as well. Assuming that λ_j are know and defining $\boldsymbol{S} = \sum_j \lambda_j \boldsymbol{S}_j$, then

$$l_p(\boldsymbol{\beta}) = l(\boldsymbol{\beta}) - \frac{1}{2}\boldsymbol{\beta}^{'}\boldsymbol{S}\boldsymbol{\beta} \tag{3.6}$$

can be maximized with respect to β_i using;

$$\begin{aligned} \frac{\partial l_p}{\partial \beta_j} &= \frac{\partial l}{\partial \beta_j} - [\boldsymbol{S}\boldsymbol{\beta}]_j \\ &= \frac{1}{\phi}\sum_{i=1}^{n} \frac{y_i - \mu_i}{V(\mu_i)} \frac{\partial \mu_i}{\partial \beta_j} - [\boldsymbol{S}\boldsymbol{\beta}]_j = 0 \end{aligned} \tag{3.7}$$

where $[.]_j$ denotes the jth row vector.

Given $\lambda_j, \hat{\boldsymbol{\beta}}$ is estimated via penalized maximum likelihood estimation by iterating the following two steps to convergence:

1. Given the current $\boldsymbol{\mu}^{[k]}$ calculate the pseudo-data $\boldsymbol{z}^{[k]}$ and weights $w_i^{[k]}$ where,

$$w_i^{[k]} = \frac{1}{V(\mu_i^{[k]})g'(\mu_i^{[k]})^2} \text{ and } z_i = g'(\mu_i^{[k]})(y_i - \mu_i^{[k]}) + \boldsymbol{X}_i\hat{\boldsymbol{\beta}}^{[k]},$$

   g is the model link function, $\boldsymbol{z}^{[k]}$ is a vector of pseudo-data and $\boldsymbol{W}^{[k]}$ is a diagonal matrix with diagonal elements $w_i^{[k]}$

2. Minimize

$$\| \sqrt{\boldsymbol{W}^{[k]}}(\boldsymbol{z}^{[k]} - \boldsymbol{X}\boldsymbol{\beta}) \|^2 + \boldsymbol{\beta}'\boldsymbol{S}\boldsymbol{\beta}$$

   with respect to $\boldsymbol{\beta}$ to find $\hat{\boldsymbol{\beta}}^{[k+1]}$. Evaluate the linear predictor $\boldsymbol{\eta}^{[k+1]} = \boldsymbol{X}\boldsymbol{\beta}^{[k+1]}$ and fitted values $\mu_i^{[k+1]} = g^{-1}(\eta_i^{[k+1]})$. Increment k.

The influence matrix of a GAM fit is $\boldsymbol{A} = \boldsymbol{X}(\boldsymbol{X}'\boldsymbol{W}\boldsymbol{X} + \boldsymbol{S})^{-1}\boldsymbol{X}'\boldsymbol{W}$, the influence matrix of the penalized working least square problem of the final step of the P-IRLS.

3.2.3 Degrees of Freedom and Residual Variance Estimation

Effective *degrees of freedom* of a GAM, defined as $tr(\boldsymbol{A})$, where $\boldsymbol{A}$ is the influence matrix described above, indicate the flexibility of the fitted model. For instance, using large values for smoothing parameters would result in a model with very few degrees of freedom which is very inflexible. The application of penalties reduces the model degrees of freedom. It is possible to break down the effective degrees of freedom of the model to each smooth function in the model or even to each $\hat{\beta}_i$ separately. It can be shown that the effective degrees of freedom for the model parameters in the general weighted case are given by the leading diagonal of $\boldsymbol{F} = (\boldsymbol{X}'\boldsymbol{W}\boldsymbol{X} + \boldsymbol{S})^{-1}\boldsymbol{X}'\boldsymbol{W}\boldsymbol{X}$, where $\boldsymbol{S} = \sum_j \lambda_j \boldsymbol{S}_j$. $\boldsymbol{F}$ can also be shown to be the matrix that maps the un-penalized estimates to the penalized ones and F_{ii} to measure the effective degrees of freedom of the ith penalized parameters.

Residual variance, σ^2 for additive model is estimated in a similar way to linear regression as

$$\hat{\sigma}^2 = \frac{\| \boldsymbol{y} - \boldsymbol{A}\boldsymbol{y} \|^2}{n - tr(\boldsymbol{A})} \tag{3.8}$$

while the scale (dispersion) parameter in case of a GAM is estimated by the Pearson-like estimator as

$$\hat{\phi} = \frac{\sum_i V(\hat{\mu}_i)^{-1}(y_i - \hat{\mu}_i)^2}{n - tr(\boldsymbol{A})} \tag{3.9}$$

3.2.4 Smoothing Parameter Selection

Penalized likelihood maximization can only estimate model coefficients, $\boldsymbol{\beta}$, given smoothing parameters $\boldsymbol{\lambda}$. This section discusses how the smoothing parameters $\boldsymbol{\lambda}$ are estimated, starting with the case of the additive model, then generalizing to GAM. Two approaches have been suggested by Wood (2006). When the scale parameter, ϕ, is known, then estimation is done by Mallow's C_p or Un-Biased Risk Estimator (UBRE). This approach is discussed in details, UBRE by Craven and Wahba (1979) and Mallow's C_p by Mallows (1973). When the scale parameter is unknown, then estimation is done using the generalized cross validation (GCV). GCV is discussed in this report.

The ordinary cross validation (OCV) criterion is based on an attempt to minimize the average mean squared error in predicting a new observation y using the fitted model. By omitting observation y_i while fitting the model, using the model to predict $E(y_i)$, and repeating the procedure to all data in turn, leads to the following estimate of OCV in the additive model case:

$$v_0 = \frac{1}{n}\sum_{i=1}^{n}(y_i - \hat{\mu}_i^{[-i]})^2 \tag{3.10}$$

where $\hat{\mu}_i^{[-i]}$ denotes the prediction of $E(y_i)$ obtained by leaving out y_i. It can be shown that estimation of v_0 does not have to proceed by fitting the model n times; indeed, it can be shown that

$$v_0 = \frac{1}{n}\sum_{i=1}^{n}\frac{(y_i - \hat{\mu}_i)^2}{(1 - A_{ii})^2} \tag{3.11}$$

which simply requires fitting the original model once. However, it has been noted that the OCV is not only computationally expensive to minimize in the additive model case where

there are several smoothing parameters but it has a *slightly disturbing lack of invariance*. The need to overcome this lack of invariance leads to the so called generalized cross validation score (GCV). In the additive model case, it is given as

$$v_g = \frac{n \parallel \boldsymbol{y} - \boldsymbol{\mu} \parallel^2}{[n - tr(\boldsymbol{A})]^2} \tag{3.12}$$

which provides a valid estimate of the prediction error just like the OCV, but has the invariance property. Generalization of the GCV criterion to the GAM case is straightforward. By first writing the GAM fitting objective in terms of model deviance,

$$D(\boldsymbol{\beta}) + \sum_{j=1}^{m} \lambda_j \boldsymbol{\beta}' \boldsymbol{S}_j \boldsymbol{\beta}$$

an applicable GCV score has been defined as

$$v_g = \frac{nD(\hat{\boldsymbol{\beta}})}{[n - tr(\boldsymbol{A})]^2} \tag{3.13}$$

Two numerical strategies suggested for estimating the smoothing parameters are the performance iteration and outer iteration. Details of these strategies are discussed in details by Wood (2006).

3.2.5 Confidence Intervals for Functions of Parameters

Having described the estimation of model parameters $\boldsymbol{\beta}$ and $\boldsymbol{\lambda}$, it is of interest to not only quantify the uncertainty surrounding them but to calculate confidence intervals for $\boldsymbol{\beta}$ as well as quantities derived from them such as the smooth terms themselves. Also of interest is to test for the need of terms in the model. Bayesian confidence intervals which follow from the Bayesian approach to uncertainty estimation are utilized. When some penalties are imposed, it implies that we are expressing our prior belief about the likely characteristics of the correct model. This leads to the concept of specifying a prior for $\boldsymbol{\beta}$. Starting with the additive model case, assume that bases and penalties have been chosen, so that the model can be written as

$$\boldsymbol{Y} = \boldsymbol{X}\boldsymbol{\beta} + \boldsymbol{\varepsilon}$$

The fitting of the model can proceed by minimizing the penalized least squares criterion

$$\parallel \boldsymbol{W}^{\frac{1}{2}}(\boldsymbol{y} - \boldsymbol{X}\boldsymbol{\beta}) \parallel^2 + \sum_{i=1}^{m} \lambda_i \boldsymbol{\beta}' \boldsymbol{S}_i \boldsymbol{\beta}$$

where $\boldsymbol{W}$ is some positive definite weight matrix. It is assumed that constraints to make the model identifiable have been resolved by re-parametrization. Let the prior for $\boldsymbol{\beta}$ be

$$f_{\beta}(\boldsymbol{\beta}) \propto \exp\left(\frac{-\frac{1}{2}\boldsymbol{\beta}'\sum \boldsymbol{S}_i}{\tau_i \boldsymbol{\beta}}\right)$$

where τ_i are parameters controlling the dispersion of the prior. This prior not only expresses belief in smooth rather than wiggly models but gives equal probabilities to all models of equal smoothness. It can be shown that the posterior distribution is

$$\boldsymbol{\beta}|\boldsymbol{y} \sim N(\hat{\boldsymbol{\beta}}, (\boldsymbol{X}'\boldsymbol{W}\boldsymbol{X} + \sum_i \lambda_i \boldsymbol{S}_i)^{-1}\sigma^2)$$

which can be used to calculate credible intervals for any quantities derived from $\boldsymbol{\beta}$. Similarly for the GAM, $g(\mu_i) = \boldsymbol{X}_i\boldsymbol{\beta}$ where $\mu_i \equiv E(Y_i), Y_i \sim$ some exponential family and g is the link function. The model is estimated by minimizing

$$-l(\boldsymbol{\beta}) + \frac{1}{2}\sum_{i=1}^{m} \lambda_i \boldsymbol{\beta}'\boldsymbol{S}_i\boldsymbol{\beta}$$

with respect to $\boldsymbol{\beta}$, where $l(\boldsymbol{\beta})$ is the models log likelihood. Similarly, it has been shown that

$$\boldsymbol{\beta}|v \sim N([\boldsymbol{X}'\boldsymbol{W}\boldsymbol{X} + \sum \lambda_i]^{-1}\boldsymbol{v}, [\boldsymbol{X}'\boldsymbol{W}\boldsymbol{X} + \sum \lambda_i]^{-1}\boldsymbol{\phi}) \text{ where } \boldsymbol{v} = \boldsymbol{X}'\boldsymbol{W}\boldsymbol{z}.$$

This then requires plugging the estimates of $\boldsymbol{v}$ and $\boldsymbol{W}$ as evaluated at convergence of the P-IRLS algorithm and an estimate of $\boldsymbol{\phi}$ if necessary, after which results can be used to approximate Bayesian confidence intervals for quantities derived from $\boldsymbol{\beta}$. It has been noted that confidence intervals for individual GAM components can be improved by accounting for the smoothing parameter uncertainty; i.e., by constructing intervals based on the joint posterior density.

$$f(\boldsymbol{\beta}, \hat{\boldsymbol{\lambda}}|\boldsymbol{y}) = f(\boldsymbol{\beta}|\hat{\boldsymbol{\lambda}}, \boldsymbol{y}) f(\hat{\boldsymbol{\lambda}}|\boldsymbol{y})$$

3.3 Generalized Additive Mixed Models (GAMM)

In situations where data consists of repeated measurements taken on each patient, the likely patient-to-patient variation introduces a new source of randomness and an extension to GAM may be necessary. Just like generalized linear mixed models (GLMM) are extensions of GLM, GAM can also be extended to GAMM (generalized additive mixed models) by inclusion of random effects.

Lin and Zhang (1999) define a generalized additive mixed model (GAMM) as simply a GLMM in which part of the linear predictor is specified in terms of smooth functions. Using the notation of Wood (2006), an additive mixed model (AMM), a special case of GAMM, has the following structure:

$$y_i = \boldsymbol{X}_i\boldsymbol{\beta} + f_1(x_{1i}) + f_2(x_{2i}, x_{3i}) + \ldots + \boldsymbol{Z}_i\boldsymbol{b} + \varepsilon_i \tag{3.14}$$

where y_i is a univariate response; $\boldsymbol{\beta}$ is a vector of fixed parameters; $\boldsymbol{X}_i$ is a row of the design matrix corresponding to the fixed-effects; $f_j(.)$ are smooth functions of covariates x_k; $\boldsymbol{Z}_i$, is a row of the design matrix corresponding to random effects, $\boldsymbol{b} \sim N(\boldsymbol{0}, \Psi_\theta)$ is a vector of random effects coefficients where Ψ_θ is positive definite with parameter θ, and $\boldsymbol{\varepsilon} \sim N(\boldsymbol{0}, \boldsymbol{\Lambda})$ is the residual error vector.

3.3.1 Estimation of GAMM

A GAMM can be readily transformed into a linear mixed model by making use of Bayesian model of smoothing discussed in Section 3.2.1. The smoothing parameters are treated as variance components to be estimated. Each smooth is considered to have a fixed effects (un-penalized) component and a random effects (penalized) component. These components are respectively absorbed into $\boldsymbol{X}_i\boldsymbol{\beta}$ and $\boldsymbol{Z}_i\boldsymbol{b}$. Consider a smooth with a single smoothing parameter

$$f(\boldsymbol{x}_i) = \sum_{j=1}^{J} b_j(\boldsymbol{x}_i)\beta_j \tag{3.15}$$

with associated *wiggliness* measure, $J(f) = \boldsymbol{\beta}'\boldsymbol{S}\boldsymbol{\beta}$, where $\boldsymbol{S}$ is a positive semi-definite matrix of coefficients. The Bayesian approach of estimating f starts on the premise that, by stating that f is smooth, we acknowledge our prior belief that f is more likely smooth than wiggly, which can be formalized by adopting a prior for how wiggly the model is. This argument can be expanded to finally show that (3.15) has a mixed model representation

$$\boldsymbol{X}_F\boldsymbol{\beta}_F + \boldsymbol{X}_R\boldsymbol{b}_R \text{ where } \boldsymbol{b}_R \sim N(\boldsymbol{0}, \boldsymbol{D}_+^{-1}/\lambda)$$

and λ and $\boldsymbol{\beta}_F$ are fixed parameters to be estimated. $\boldsymbol{D}_+$ denotes a sub-matrix of a matrix $\boldsymbol{D}$ which is involved in the eigen-decomposition of $\boldsymbol{S}$. This can further be re-parameterized to:

$$\boldsymbol{X}_F\boldsymbol{\beta}_F + \boldsymbol{Z}\boldsymbol{b} \text{ with } \boldsymbol{b} \sim N(\boldsymbol{0}, \boldsymbol{I}/\lambda)$$

3.3.2 Inference with GAMM

The Bayesian approach is can be in evaluating credible regions for the smooth components. It has be shown that the Bayesian approach implies:

$$\boldsymbol{\beta} \sim N(\hat{\boldsymbol{\beta}}, (\bar{\boldsymbol{X}}^{'}\boldsymbol{V}^{-1}\bar{\boldsymbol{X}} + \boldsymbol{S})^{-1})$$

where $\boldsymbol{S} = \sum \lambda_i/\sigma^2 \boldsymbol{S}_i$, $\boldsymbol{V} = \bar{\boldsymbol{Z}}\Psi_\theta\bar{\boldsymbol{Z}}^{'} + \boldsymbol{\Lambda}\sigma^2$ where $\bar{\boldsymbol{Z}}$ is the random effects model matrix excluding the columns relating to smooths, Ψ_θ is the corresponding random effects covariance matrix, $\boldsymbol{\beta}$ contains all the fixed effects and the random effects of the smooth terms (only) and $\bar{\boldsymbol{X}}$ is the corresponding model matrix. The effective degrees of freedom for each element of $\boldsymbol{\beta}$ are given by the leading diagonal of

$$\boldsymbol{F} = (\bar{\boldsymbol{X}}^{'}\boldsymbol{V}^{-1}\bar{\boldsymbol{X}} + \boldsymbol{S})^{-1}(\bar{\boldsymbol{X}}^{'}\boldsymbol{V}^{-1}\bar{\boldsymbol{X}})$$

Inference for the AMM can proceed in a manner similar to that of linear mixed models.

3.4 Software

Data manipulation and exploratory data analysis were performed using Statistical Analysis Software (SAS, version 9.2) while are graphical presentations and statistical analysis were done using CRAN-R (version 2.13.1). Selected codes are shown in Appendix: A.1 for SAS and Appendix: A.2 for R. All statistical tests were conducted at $\alpha = 0.05$ level of significance.

4 Results

4.1 Summary Statistics

Patients were classified into two groups with 4 belonging to survivor group and 8 to non-survivor groups. Means and variance of cerebral oxygen saturation for each patient were computed for each phase and are shown in Table 1. In the cooling phase, variability was highest in patient CCU02 and smallest in patient CCU05. In the hypothermia, rewarming and normothermia phases, variability was highest in patients CCU04, CCU01, and CCU07 and smallest in patients CCU11, CCU06, and CCU05 respectively. The high variability for patients CCU04 and CCU12 was observed during the hypothermia phase and it ia attributed to the two patient deaths.

Table 1: Means and variances of cerebral oxygen saturation for each patient

	Cooling		**Hypothermia**		**Rewarming**		**Normothermia**	
Patient	Mean	Variance	Mean	Variance	Mean	Variance	Mean	Variance
CCU01	65.17	15.37	65.09	6.09	72.75	18.78	72.79	3.23
CCU02	59.19	59.38	63.95	18.94	76.11	15.96	74.38	10.31
CCU03	62.79	38.17	72.12	15.31	77.46	5.15	71.49	11.88
CCU04	60.31	4.02	50.63	149.88	-	-	-	-
CCU05	59.92	1.68	59.61	18.96	64.16	1.34	64.76	1.09
CCU06	69.57	24.32	73.22	5.56	73.26	0.36	73.31	6.98
CCU07	67.89	24.87	70.89	3.06	77.99	9.33	76.27	15.20
CCU08	65.43	11.84	67.57	30.52	72.10	3.14	74.35	4.86
CCU09	58.88	20.80	61.68	5.26	64.13	3.47	68.03	2.26
CCU10	64.77	27.97	66.89	35.59	75.82	1.97	72.31	9.33
CCU11	63.63	10.56	62.47	1.69	62.01	2.75	67.79	3.21
CCU12	59.51	21.65	53.88	52.52	-	-	-	-

Absolute values representing variability of cerebral oxygen saturation in each phase were computed for each patient group as shown in Table 2. The lowest measurement (26.5) was observed in the hypothermia phase for non-survivor group. This measurement is from one of the patients who died during the study. The highest measurement (94.0) was observed during the Normothermia phase for non-survivor group also. Other measurements were found to lie inside this range. Measurements observed during the cooling and hypothermia phases were smallest in value whereas those observed during rewarming and normothermia phases where largest. Variability was smallest in the normothermia phase and largest in the hypothermia phase.

Table 2: Summary statistics for cerebral oxygen saturation

Phase	Patient group	Mean	Std. Dev.	Minimum	Maximum
Cooling	Survivor	64.11	5.684	52.0	81.5
	Non-survivor	64.11	6.541	47.5	82.0
Hypothermia	Survivor	67.12	6.429	51.5	83.5
	Non-survivor	63.82	6.865	26.5	82.0
Rewarming	Survivor	71.93	5.505	61.5	85.5
	Non-survivor	71.51	6.615	53.5	89.0
Normothermia	Survivor	69.80	4.309	58.5	87.0
	Non-survivor	71.90	4.330	50.0	94.0

Summary statistics for other parameters in each phase were computed for each patient group as shown in Table 3. Generally, measurement from survivor group were more variable than those from non-survivor group partly due to the small sample size in that group.

In the cooling phase, it was observed that, oesophagale temperature appeared comparable in both patient groups but more variable in survivor group. Rectal temperature appeared to be slightly higher in non-survivor group, but more variable in survivor group. CCO was slightly higher and more variable in survivor group. CO2 content was also comparable across both groups, although it was more variable in non-survivor group. pO2 was larger and more variable in non-survivor group.

In the hypothermia phase, it was observed that, oesophagale temperature was slightly higher and more variable in survivor group. Rectal temperature was slightly higher and more variable in non-survivor group. CCO and CO2 were higher and more variable in survivor group. pO2 was larger and more variable in non-survivor group.

In the rewarming phase, it was observed that, oesophagale and rectal temperatures were comparable across both groups. CCO was slightly higher and more variable in survivor group. CO2 larger in survivor group but more variable in non-survivor group. O2 was larger in non-survivor group but more variable in survivor group.

In the normothermia phase,it was observed that, oesophagale temperature comparable in both groups, but slightly variable in non-survivor group. Rectal temperature was slightly higher in non-survivor group, but more variable in survivor group. CCO was higher and more variable in survivor group. CO2 was higher in non-survivor group, but more variable in survivor group. pO2 was larger and more variable in non-survivor group.

Table 3: Summary statistics for other parameters

Phase	Parameter	Patient group	Mean	Std. Dev.	Min.	Max.
Cooling	Oesophagale	Survivor	34.02	0.94	33.1	36.2
		Non-survivor	34.07	0.71	33.1	36.1
	Rectal	Survivor	34.13	0.81	32.9	36.3
		Non-survivor	35.05	0.76	32.9	36.5
	CCO	Survivor	3.29	0.73	2.5	6.0
		Non-survivor	3.64	0.99	2.0	5.9
	CO2	Survivor	44.25	8.38	33.4	62.0
		Non-survivor	43.87	13.18	19.2	74.1
	pO2	Survivor	102.69	36.70	33.4	169.0
		Non-survivor	136.96	97.02	19.2	652.0
Hypothermia	Oesophagale	Survivor	33.16	0.45	31.85	35.1
		Non-survivor	33.02	0.32	27.93	34.1
	Rectal	Survivor	33.29	0.51	32.3	34.5
		Non-survivor	34.01	0.71	30.4	34.9
	CCO	Survivor	6.07	1.50	2.3	11.1
		Non-survivor	5.42	0.95	1.9	7.3
	CO2	Survivor	42.38	9.63	28.5	64.2
		Non-survivor	37.71	7.55	23.1	75.6
	pO2	Survivor	96.84	21.80	45.8	154.0
		Non-survivor	100.20	23.03	34.9	182.0
Rewarming	Oesophagale	Survivor	35.00	1.06	33.08	37.0
		Non-survivor	34.88	1.01	32.74	37.3
	Rectal	Survivor	35.18	1.12	32.9	37.3
		Non-survivor	35.97	1.06	33.5	37.4
	CCO	Survivor	6.67	0.91	3.1	11.67
		Non-survivor	5.60	0.64	2.4	8.4
	CO2	Survivor	39.53	6.50	26.4	54.5
		Non-survivor	37.39	7.77	25.7	74.1
	pO2	Survivor	83.34	18.60	35.9	146.0
		Non-survivor	85.51	16.19	29.0	155.0
Normothermia	Oesophagale	Survivor	37.06	0.20	36.65	37.94
		Non-survivor	36.79	0.45	35.87	38.28
	Rectal	Survivor	37.31	0.48	33.9	38.1
		Non-survivor	39.05	0.35	35.4	39.6
	CCO	Survivor	7.63	1.34	3.71	12.68
		Non-survivor	5.79	0.85	3.4	9.6
	CO2	Survivor	36.48	5.99	26.4	56.2
		Non-survivor	38.35	4.95	29.6	63.6
	pO2	Survivor	83.89	14.47	34.6	125.0
		Non-survivor	90.82	20.86	36.1	156.0

Additionally, some patients did not have measurements for some parameters due to lack of enough monitoring equipments and thus they did not contribute to these results.

4.2 Individual Profiles

To get a glimpse of the evolution of cerebral oxygen saturation, individual patient profiles were plotted as shown in Figure 1.

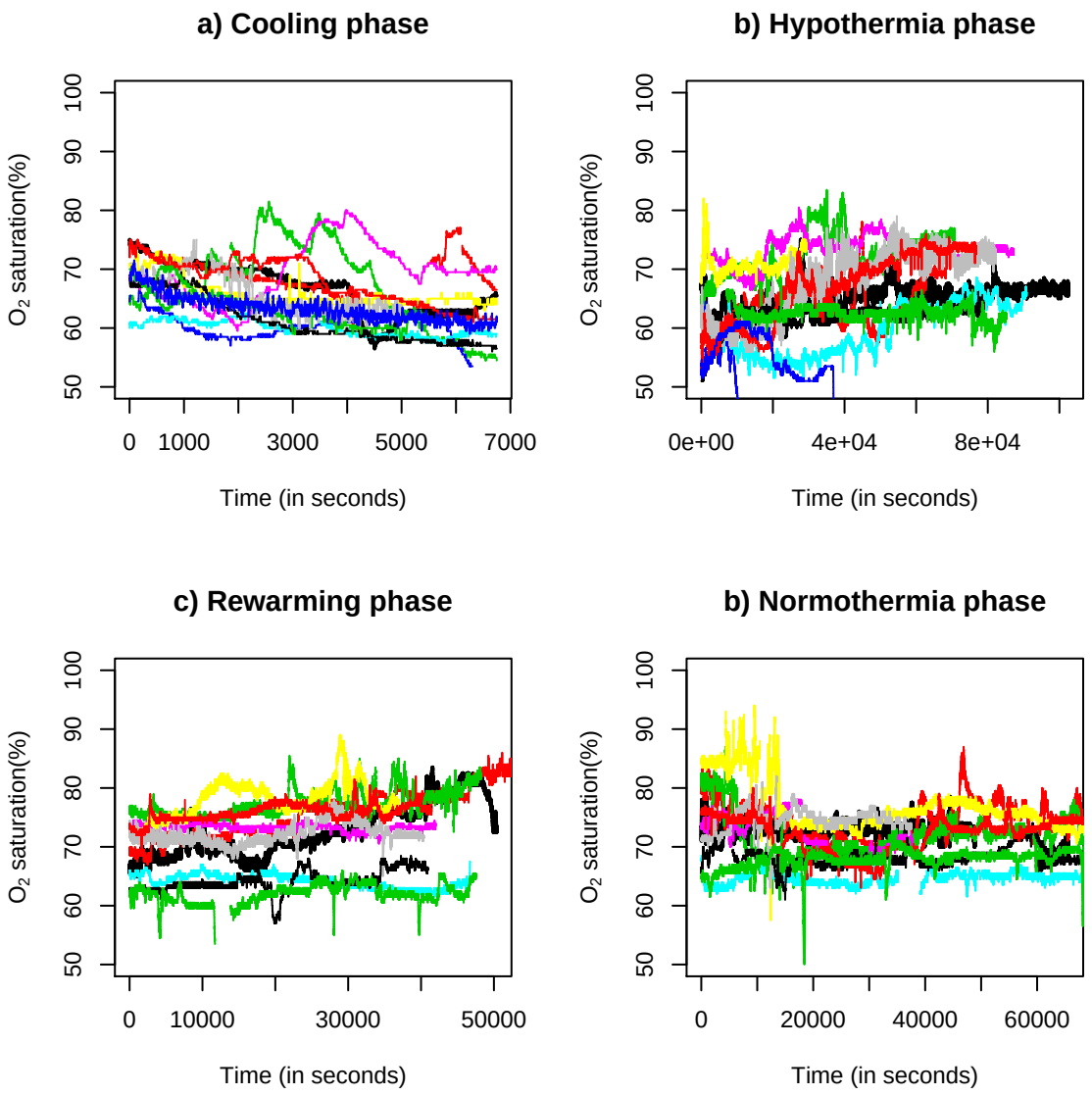

Figure 1: Individual profiles of cerebral oxygen saturation over time

Generally, trend was seen to mimic temperature regulations performed in each phase. For instance, a decreasing trend in the cooling phase was observes with lowering patient's body temperature. Differences in evolution over time were noted in each phase, suggesting use of random effects. Individual profile fluctuations indicated presence of within-patient variability.

4.3 Mean Structure

In order to be able to further visualize overall evolution of cerebral oxygen saturation, averages were computed at each time point and plotted against time as shown in Figure 2 (a-d).

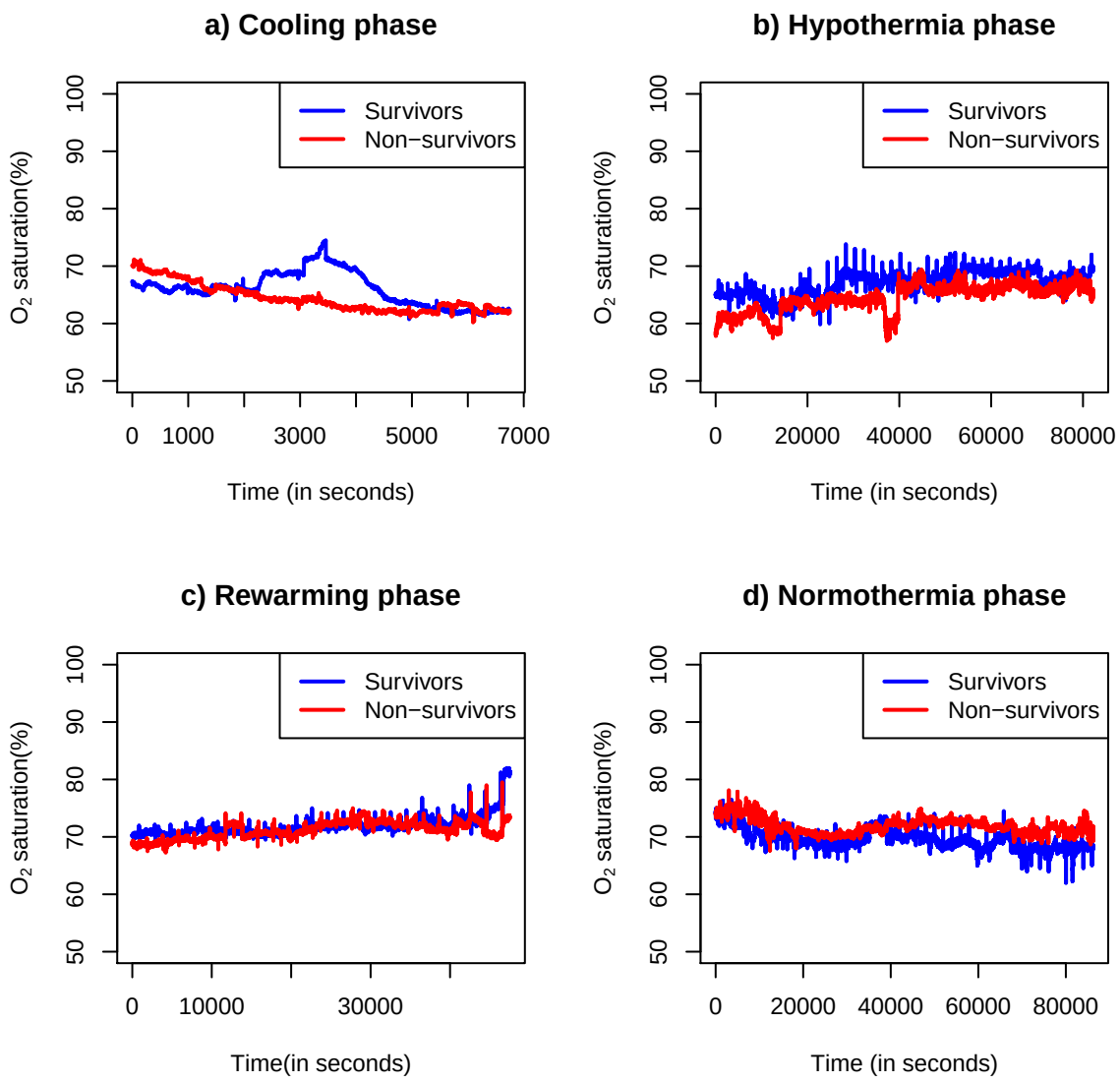

Figure 2: Average evolution of cerebral oxygen saturation over time

In the cooling phase, cerebral oxygen saturation on average started at a lower values in survivor group compared to non-survivor group. It gradually increased reaching a maximum peak after about 3500 seconds, before starting to decrease towards baseline. In non-survivor group, there was a gradual decrease over time. In the hypothermia phase, oxygen saturation on average started at higher values in survivor group than non-survivor group and remained

higher throughout the phase. In the rewarming phase, cerebral oxygen saturation on average appeared constant over time with the two curves overlapping one another. In the normothermia phase, cerebral oxygen saturation on average started at higher values in non-survivors than survivors and remained higher throughout the phase.

4.4 Variance Structure

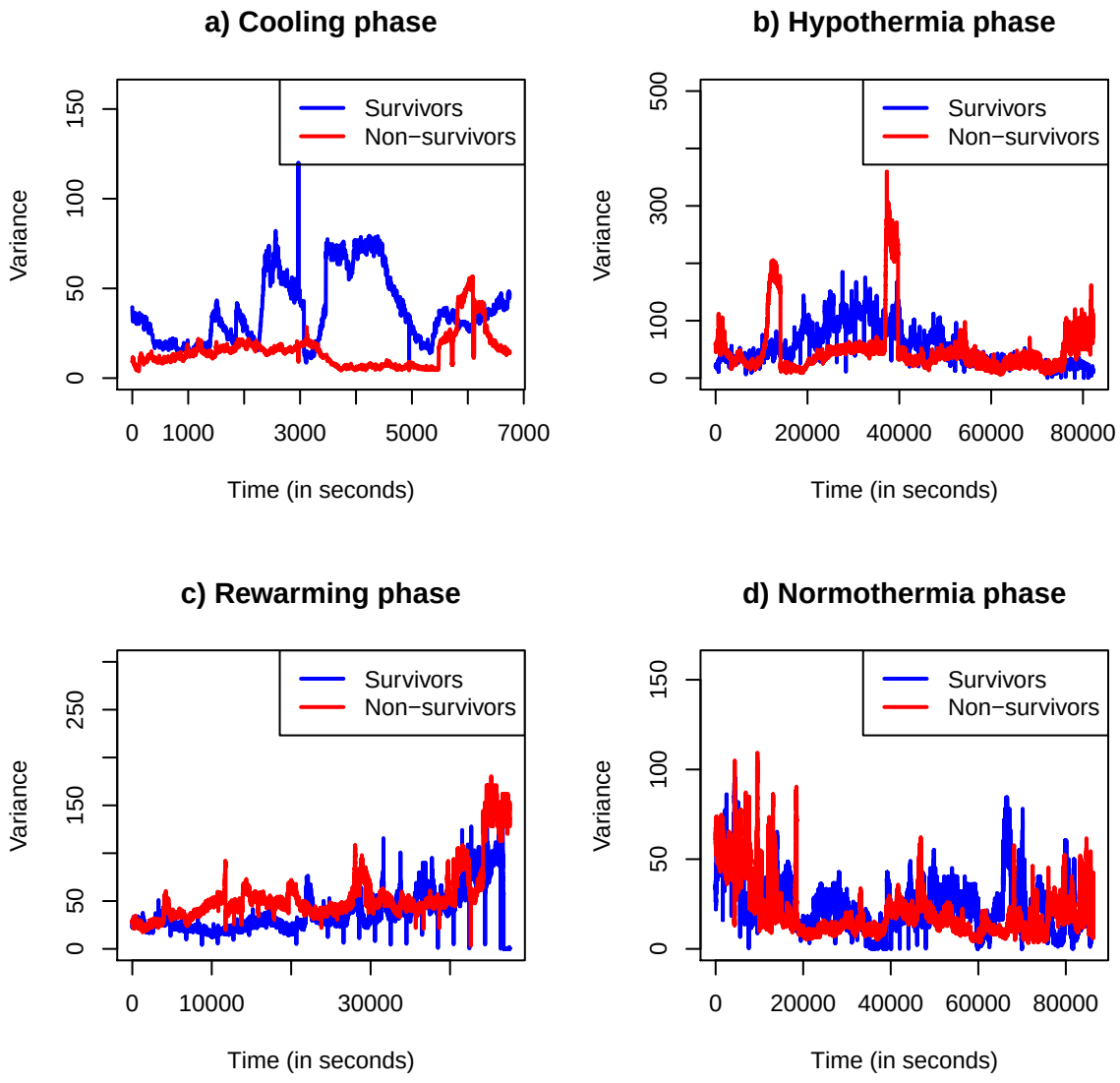

Figure 3: Variability of cerebral oxygen saturation over time

To study the variability over time, cerebral oxygen saturation variance in each phase was computed for each patient at each time point and then plotted against time. Figure 3 presents

variance functions, indicating variability in each phase and patient group.

In the cooling phase, cerebral oxygen saturation was more variable in survivor group compared to non-survivor group. This was attributed partly to small sample size ($N = 4$) for that group. In the hypothermia phase, variability for non-survivor group was generally higher at the start of the series, but appeared to level up with that of survivor group during late time points. In the rewarming phase, variability increased over time but remained higher in non-survivor group most of the time. In the normothermia phase, variability was high at the start of the series in both patient groups, but appeared to stabilize after 20000 seconds.

4.5 Correlation Structure

In order to be able to study the correlations in each phase, Pearson correlations cerebral oxygen saturation and other parameters were computed between and the corresponding correlation matrices plotted as shown in Figure 4 (a-d).

Values marked with an (*) indicate that correlations, which measures the linear association between two variables, were significant at $\alpha = 0.05$ level of significance. Plots indicate a graphical representation of the best predicted linear or non-linear association between two variables. It was observed that most correlations were fairly strong, but highly significant.

In the cooling, hypothermia, rewarming and normothermia phases, the highest correlations were respectively 0.61, 0.58, 0.95, and 0.11 and were between oesophagale and rectal temperatures. They were also significant as expected since both variables measure body temperature.

In the cooling phase, the smallest correlation was -0.012 and was between cerebral oxygen saturation and oesophagale temperature. However, this was counter-intuitive since body temperature and oxygen saturation were both expected to decrease over time, but could be attributed partly due to the small sample.

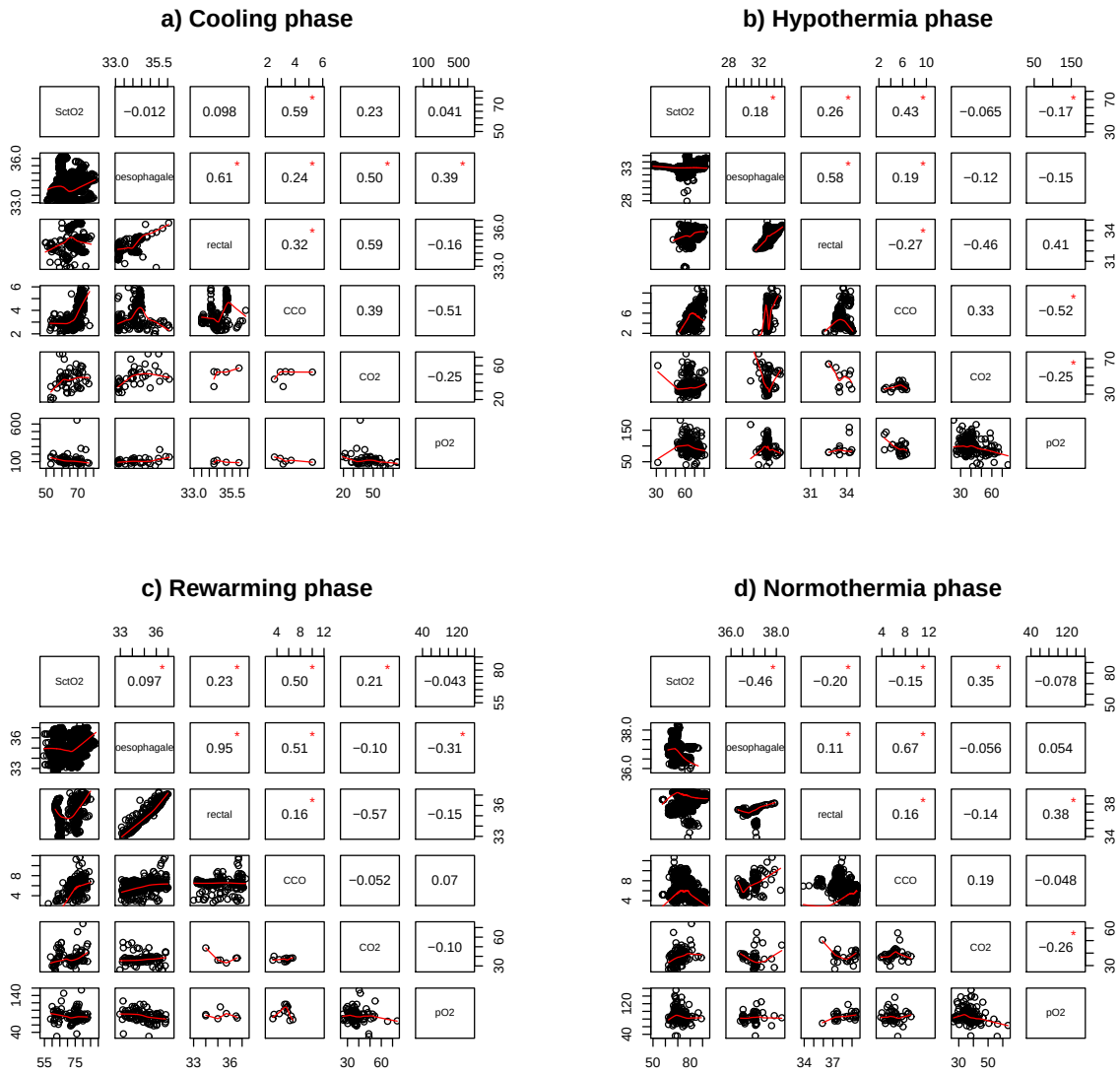

Figure 4: Correlation in each phase

In the hypothermia phase, the smallest correlations was -0.065 and was observed between cerebral oxygen saturation and carbon dioxide content in the blood. In the rewarming phase, the smallest correlations was -0.043 and was observed between cerebral oxygen saturation and oxygen content in the blood. In the normothermia phase, the smallest correlations was -0.048 and was observed between cardiac output and oxygen content in the blood.

Generally, all the smallest correlations were also not significant (p-$value$ >0.05)

4.6 Statistical Model

To be able to estimate cerebral oxygen saturation trend over time in each phase and for each patient group, the following preliminary additive model was fitted

$$SctO2_{ijk} = f_1(time_k) + f_2(time_k)group_j + patient_i + \varepsilon_{ijk} \tag{4.1}$$

where, for $i = 1, \ldots, 12, j = 1, 2, k = 0, \ldots, N$,
$SctO2_{ijk}$ is the cerebral oxygen saturation measurement k of patient i belonging to group j.
$f_1(.)$ is a smooth function representing trend for non-survivor group.
$f_2(.)$ is a *correction* or *difference* curve representing the smooth effect of survival.
$group_j$ is a dummy variable indicating patient group.
$patient_i$ is the random effect of patient i.
ε_{ijk} is the random error for measurement k of patient i belonging to group j.
It is assumed that $patient_i \sim N(0, \sigma_p^2)$ and $\varepsilon_{ijk} \sim N(0, \sigma^2)$.

Both smooth functions were represented using cubic regression splines. Implementation of the model using entire profiles of repeated measurements for each patient was not possible in the cooling phase because of a number of issues present in the data. Firstly, one patient had a very large profile of repeated measures compared to the rest. Caiado et al. (2006) suggested two methods of dealing with this. The first involves extrapolating the shorter series to match the longer one. This method however, does not produce desirable results when the length difference is very large such as the case in this study. The other approach involves reducing the larger series to match the smaller series. Though it involves truncating data, it has the advantage of constructing an appropriate test. The second approach was therefore applied in this report leading to reduced profiles of length of 6750 seconds (225 minutes).

Secondly, due to large number of profiles, there was limitation of computer memory available for use by the software which could not be solved even by increasing memory requirements to the maximum (4Gb) available. Two solutions were suggested. The first one was to reduce the number of profiles to a level that could allow implementation. The second one was to aggregate measurements over the minute-time interval. Though both methods involves reducing the number of profiles, the second one has an advantage that the entire profile length is used and was thus applied to measurements in each phase.

Results from *gam* component in the cooling phase, are shown in Table 4. Trend for non-survivors was estimated as a smooth curve with 6.790 degrees of freedom, while the *correction* or *difference* curve representing smooth effect of survival was estimated to have 9.684 degrees

of freedom. In total, estimated model had 17.474 degrees of freedom (1 degree of freedom for model intercept inclusive). Approximate p-value, corresponding to the correction term, was <.0001, and gave a clear-cut evidence for a significant additive effect of patient group.

The selected model also provided a better fit than a simpler model without the correction term. This was concluded by comparing Akaike Information Criterion (AIC) values obtained from *lme* components of both models, which were equal to 9757.862 and 10323.452 respectively. Thus, likelihood-based approach also provided support for the model including the correction term. Adjusted R^2 for this model was 0.487 implying the model explained about 48.7% of total variability in the data. Variance components were estimated as; *residual variance*, $\sigma^2 = 8.15$ and *random effects variance*, $\sigma_p^2 = 9.74$ an indication that there was high patient-to-patient variability.

Table 4: Model results from GAM component

Function	**Estimated df**	**F**	**p-value**	**Adjusted R^2**
$f_1(time_k)$	6.790	404.94	<.0001	0.487
$f_2(time_k)group_j$	9.684	76.32	<.0001	

AIC-based approach was also used to assess whether or not selected model, in which the effect of patient group over time was captured in a smooth manner, provided a better fit than an alternative model, which assumed that the effect was constant over time. Respective AIC values were 9757.862 and 10324.325, clearly supporting the former over the latter. Attempts to fit models with higher order random time effects were not successful due to computer memory limitations.

Having inferred a significant effect of patient group, it was of interest to find out the exact portions along the oxygen saturation profile, where patient group had a significant effect, and to detect what type of effect it was. This was achieved by considering the smooth correction term with its credible intervals.

Figure 5 (a-b) shows estimated smooth functions in each patient group. The solid lines represent estimated trend while the dashed lines show 95% Bayesian credible intervals. Time values (in minutes) are shown on the x-axis of the plots, and estimated smooth function on the y-axis. It was observed that estimated trend for survivor group started as lower values than non-survivor group, but increased to reach a maximum peak. It then decreased gradually over time reaching a minimum peak and then started to increase towards baseline values. Estimated trend for non-survivor group on the other hand was observed to reduce gradually over time. These results are in agreement with results shown in Section 4.3 and also researchers'

expectations. Additionally, estimated trend for survivor group appeared more variable than for non-survivor group as indicated by wider credible intervals. This was partly attributed to small sample size $N = 4$ for this group.

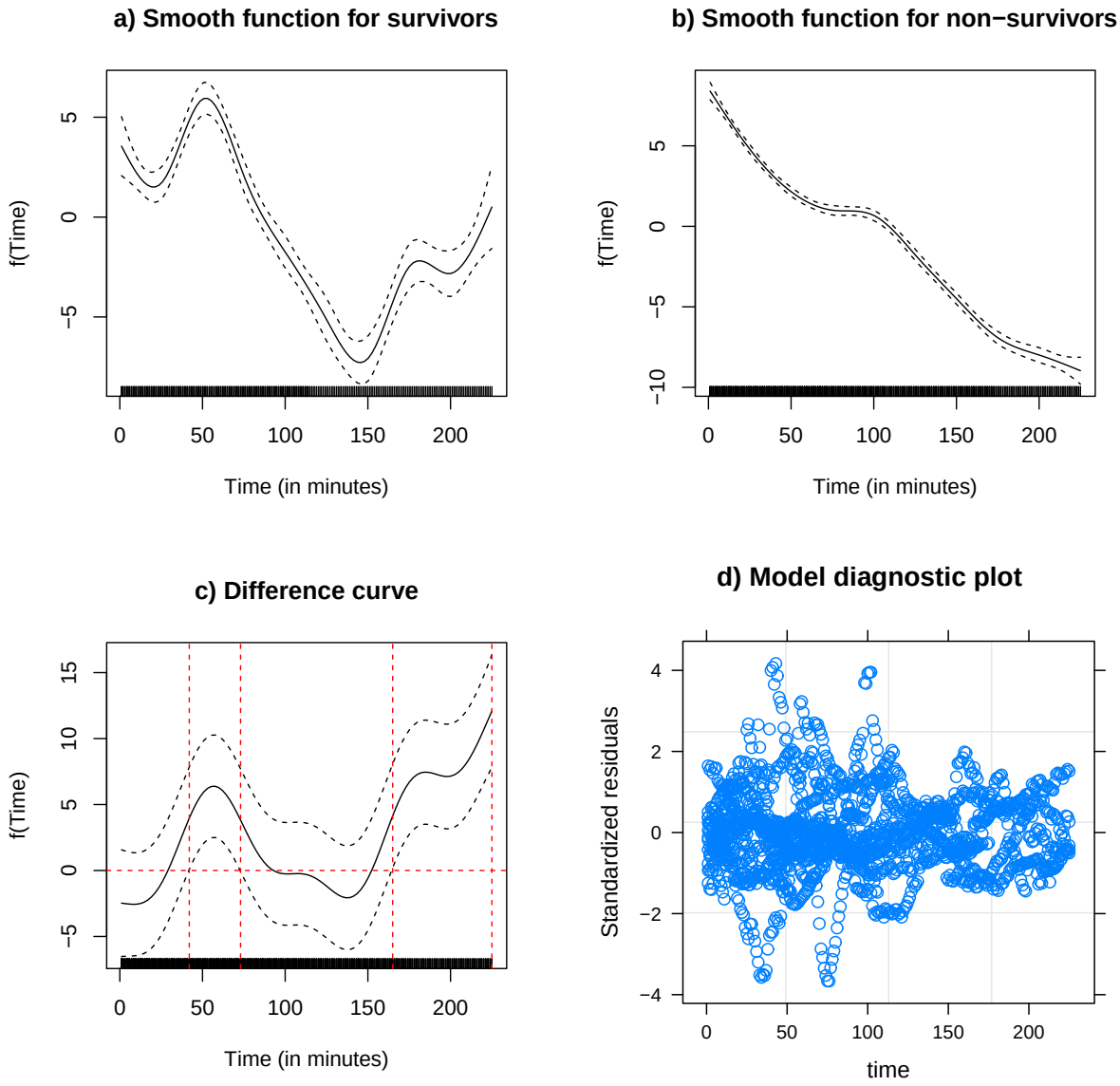

Figure 5: Estimated trend for survivor and non-survivor groups, difference curve and model diagnostics

Figure 5 (c) shows the *correction* curve representing the marginal difference of cerebral oxygen saturation over time between the two patient groups. The vertical dashed *red* lines show start and end time point intervals where estimated trend for both groups was significantly different. The first interval was $[43; 72]$ minutes and the second $[165; 225]$ minutes. In both in-

tervals, survivor group had higher measurements on average, compared to non-survivor group.

To be able to perform model diagnostics, a plot of standardized residuals versus time was plotted as shown in Figure 5 (d). Residuals were observed to scatter without showing any particular trend, an indication that selected model fitted well.

Attempts were made to estimate difference curves in other phases. Results are shown in Figure 6 (a-c).

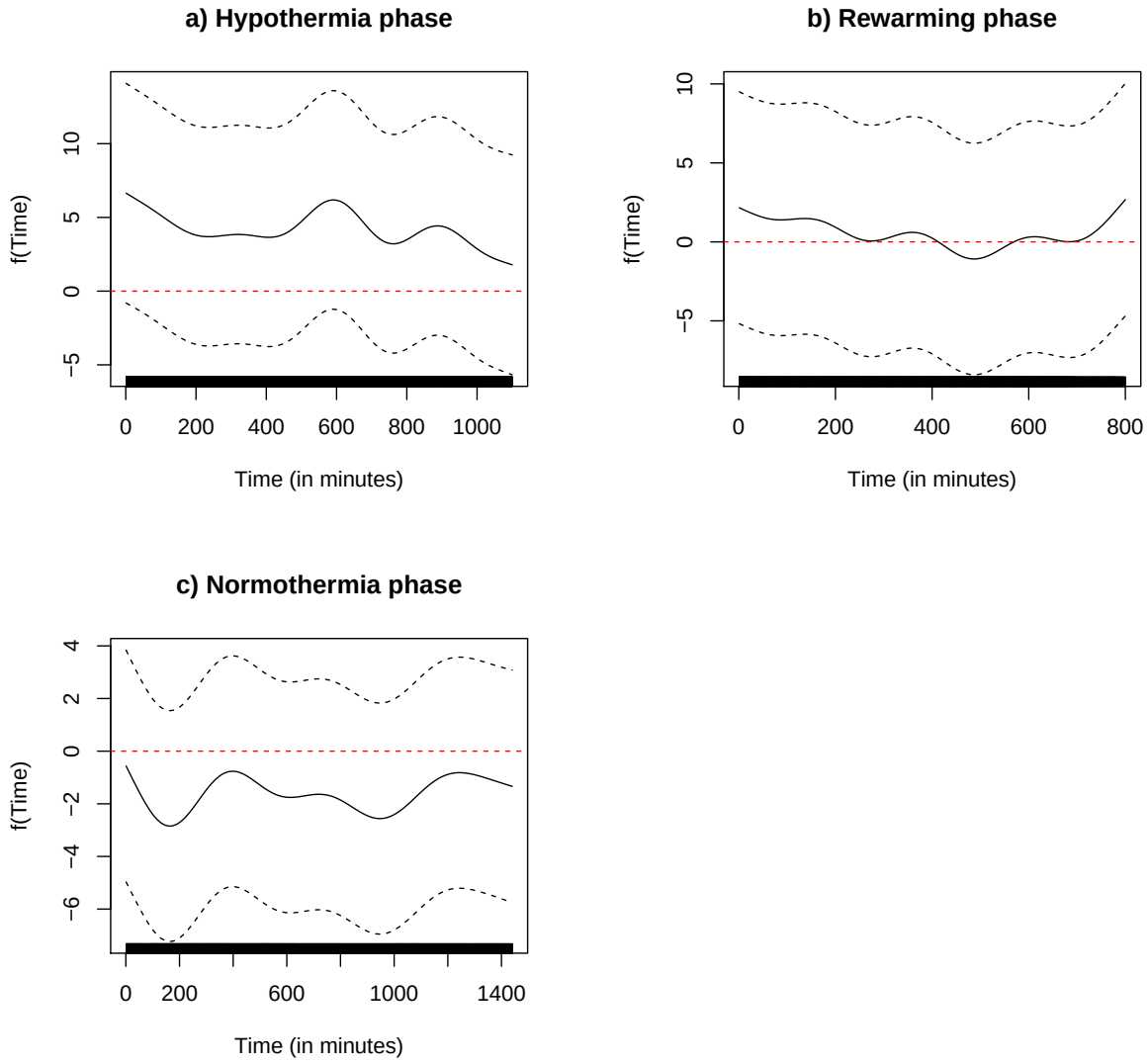

Figure 6: Estimated difference curves for other phases

The solid black line represents estimated difference curves between survivors and non-survivors.

The dashed black lines below and above estimated difference curve represent the corresponding credible interval. As expected, no significant differences in cerebral oxygen saturation trend were observed between the two patient groups.

5 Discussion

This report aimed at analyzing data collected from post-cardiac arrest patients who were put on therapeutic hypothermia. The therapy was divided into 4 phases; cooling, hypothermia, rewarming and normothermia. Patients were further divided into two patient groups; survivor and non-survivor groups. The research questions were to investigate trend and variability of cerebral oxygen saturation, and compute its correlation with other parameters in each phase. Due to highly unbalanced time series lengths in the cooling phase, some profiles were shortened leading to reduced profiles of maximum length of 6750 seconds (225 minutes) for each patient.

Individual patient variability of cerebral oxygen saturation over time around the mean were computed as shown in Table 1. High variability in the hypothermia phase for patients CCU04 and CCU12 were attributed to the said patient's death. Absolute values of variability of cerebral oxygen saturation in each patient group were computed as shown in Table 2. Variability in survivor group was lower compared to non-survivor group in all phases. Variability over time was estimated and presented in Figure 3. Generally, variability was not constant over time in all phases and for all patient groups. In the cooling phase, for instance, cerebral oxygen saturation appeared more variable in survivor group compared to non-survivor group. In other phases, variability appeared comparable over time in both patient groups, though non-constant.

Correlations between cerebral oxygen saturation and other parameters was investigated by computing Pearson's correlation as shown in Figure 4. Both significant positive and negative correlations were observed, though they were fairly strong. The correlation between cerebral oxygen saturation measurements in the right and left brain sectors in the cooling phase was found to be 0.94 ($p - value =< 0.0001$). This was expected because these are measurements from the same patient. Corresponding correlations in the hypothermia, rewarming and normothermia phases were respectively 0.94, 0.90 and 0.69. Peng and Dominici (2008) suggested that when multiple time series are observed for same parameter belonging to a single patient, they can be aggregated into a single measurement. Using this suggestion and the presence of high correlations, cerebral oxygen saturation measurement from the left and right brain sectors were aggregated into a single response. Correlation between oesophagale and rectal temperatures were found to be highly significant (p-$value$ <0.05). This is in agreement with

researcher's expectations.

According to Hill and Lewicki (2007), just like in most other analyzes in time series analysis, it is assumed that the data consists of a systematic pattern (usually a set of identifiable components) and random noise (error) which usually make the pattern difficulty to identify. Most time series analysis techniques involve some form of filtering out noise in order to make the pattern more salient. In this report, trend of cerebral oxygen saturation for both patient groups was estimated using GAMM. Results from the cooling phase shown in Figure 5 (c) indicated that estimated trend was significantly higher in survivor group compared to non-survivor group in the time intervals $[43; 72]$ and $[165; 225]$ minutes. Estimated total effective *degrees of freedom* were 17.474 for selected model. Model selection was done by fitting a number of plausible models and selecting the best fitting based on AIC values. When similar analysis was performed in other phases, no significant differences in cerebral oxygen saturation were found to exist between the two patient groups. Between-patient variability was found to be larger compared to within-patient variability.

6 Conclusion

In conclusion, it is worthy mentioning that a number of challenges, mainly surrounding the data, were encountered during the analysis. Firstly, the hospital did not have enough equipment for monitoring oesophagale temperature and therefore, some patients did not have measurements for this parameter recorded. Secondly, the sample size was very small compared to the number of repeated measures. This means that parametric methods such as linear mixed model would not be appropriate because they would require more parameter than the sample size. This prompted for use of semi-parametric models such as GAM which estimate trend using smooth functions in place of parametric terms. Thirdly, due to highly unbalanced time series in the cooling phase, some longer series were reduced by truncation to match the shorter series. Though it involved data reduction, it had the advantage of constructing appropriate tests. Lastly, even with reduced time series, it was still not possible to implement model fitting process. This led to data aggregation by averaging measurements over minute-time interval into a single measurement. Though is involved further data reduction, it has the advantage that analysis was done for the whole measurement profiles under investigation.

As a recommendation, researchers could consider possibility increasing sample size and/or using other statistical methods that are able to handle these challenges.

References

Caiado, J., Crato, N., and Penã, D. (2006). A periodogram-based metric for time series classification. *Computational Statistics & Data Analysis*, 50(10):2668-2684.

Craven, P. and Wahba, G. (1979). Smoothing noisy data with spline functions. *Numerische Mathematik*, 31(4):377-403.

Diggle, P., Heagerty, P., Liang, K., and Zeger, S. (2002). *Analysis of Longitudinal Data.* Oxford University Press, Inc., New York.

Dominici, F., McDermott, A., Zeger, S. L., and Samet, J. M. (2002). On the use of generalized additive models in times-series studies of air pollution and health. *American Journal of Epidemiology*, 156(3):193-203.

Gilks, W. R., Richardson, S., and Spiegelhalter, D. J. (1996). *Markov Chain Monte Carlo in Practice.* Chapman & Hall/CRC, London.

Harville, D. A. (1974). Bayesian inference for variance components using only error contrasts. *Biometrika*, 61(2):383-385.

Hastie, T. J. and Tibshirani, R. J. (1990). *Generalized Additive Models.* Chapman & Hall, London.

Hill, T. and Lewicki, P. (2007). *Statistics: Methods and Applications.* StatSoft, Tulsa, OK.

Holzer, M. (2002). Mild hypothermia to improve the neurologic outcome after cardiac arrest. *New England Journal of Medicine*, 346(8):549-556.

Laird, N. M. and Ware, J. H. (1982). Random-effects models for longitudinal data. *Biometrics*, 38(4):963-974.

Lin, X. and Zhang, D. (1999). Inference in generalized additive mixed models using smoothing splines. *Journal of the Royal Statistical Society. Series B (Statistical Methodology)*, 61(2):381-400.

Mallows, C. L. (1973). Some comments on Cp. *Technometrics*, 15(4):661-675.

Molenberghs, G. and Verbeke, G. (2005). *Models for Discrete Longitudinal Data.* Springer, New York.

Neuhaus, J. M., Hauck, W. W., and Kalbfleisch, J. D. (1992). The effects of mixture distribution specification when fitting mixed-effects logistic models. *Biometrika*, 79:755-762.

Peng, R. D. and Dominici, F. (2008). *Statistical Methods for Enviromental Epidemiology with R: A Case Study in Air Pollution and Health.* Springer, New York.

Ruppert, D., Wand, M. P., and Carroll, R. J. (2003). *Semiparametric Regression.* Cambridge University Press, Cambridge.

Schwartz, J., Spix, C., Touloumi, G., Bacharova, L., Barumamdzadeh, T., le Tertre, A., Piekarksi, T., Ponce de Leon, A., Ponka, A., Rossi, G., Saez, M., and Schouten, J. P. (1996). Methodological issues in studies of air pollution and daily counts of deaths or hospital admissions. *Journal of Epidemiology and Community Health*, 50(1):S3-S11.

So, H. (2010). Therapeutic hypothermia. *Korean Journal of Anesthesiology*, 59(5):299-304.

Verbeke, G. and Molenberghs, G. (2000). *Linear Mixed Models for Longitudinal Data.* Springer-Verlag, New York.

Winslow, R. (2009). How ice can save your life. *Wall Street Journal.*

Wood, S. N. (2006). *Generalized Additive Models: An Introduction with R.* Chapman & Hall/CRC, Florida.

Xiang, D. (2002). Fitting generalized additive models with the GAM procedure in statistics, data analysis, and data mining. *SUGI Proceeding.*

Appendices

A Selected SAS and R Codes

A.1 SAS Code

```
/* Import data from excel files of each patient */

PROC IMPORT OUT = WORK.coolccu01 DATAFILE = "C:\Thesis\Data\cool.xls"
DBMS = EXCEL REPLACE; RANGE = "CCU01$"; GETNAMES = YES; MIXED = NO;
      SCANTEXT = YES; USEDATE = YES;SCANTIME = YES; RUN;

/* Average left and right brain SctO2 measurements */

data coolccu01; set coolccu01; patient = "CCU01";
coolSctO2 = (coolSctO2left + coolSctO2right)/2;
if coolSctO2left =. then coolSctO2 = coolSctO2right;
if coolSctO2right =. then coolSctO2 = coolSctO2left; run;

/* Merge data and allocate patient group */

data coolall; set coolccu01 coolccu02 coolccu03 coolccu04
coolccu05 coolccu06 coolccu07 coolccu08 coolccu09 coolccu10
coolccu11 coolccu12; group=0;
if patient="CCU01"|patient="CCU03"|patient="CCU05"|patient="CCU06"
then group=1; by time patient; run;

/* Summary statistics for each patient */

proc univariate data = coolall;
var coolSctO2 cooloesophagale coolrectal coolCCO coolCO2 coolpO2;
by patient; run;

/* Summary statistics for each patient group*/

proc univariate data = coolall;
var coolSctO2 cooloesophagale coolrectal coolCCO coolCO2 coolpO2;
by group; run;

/* Data aggregation over minute-time interval for each patient */

/* CCU01 */

data temp01; do i = 1 to 227; do j = 1 to 30;
ObsID = j; output; end; end; run;
```

```
data cooltemp01;merge temp01 coolccu01;if time ne. then output;run;

proc summary data = cooltemp01 nway; output out = coolccu01summ
mean(coolSctO2) = SctO2 mean(cooloesophagale) = oesophagale
mean(coolrectal) = rectal mean(coolCCO) = CCO mean(coolCO2) = CO2
mean(coolpO2) = pO2; by i; run;

data coolccu01summ; set coolccu01summ; time = i; run;

/* Merge aggregated data */

data coolaggr; set coolccu01summ coolccu02summ coolccu03summ
coolccu04summ coolccu05summ coolccu06summ coolccu07summ
coolccu08summ coolccu09summ coolccu10summ coolccu11summ
coolccu12summ; group=0;
if patient="CCU01"|patient="CCU03"|patient="CCU05"|patient="CCU06"
then group=1; by time patient; run;
```

A.2 R Code

```
# Set data path
data_path=("C:/Thesis/Data");setwd(data_path)

# Import data for use in EDA
cool=read.table("coolReda.txt",header=TRUE,sep=" ")
hypo=read.table("hypoReda.txt",header=TRUE,sep=" ")
rewarm=read.table("rewarmReda.txt",header=TRUE,sep=" ")
normo=read.table("normoReda.txt",header=TRUE,sep=" ")

##############################################################
#                        Mean Structure                      #
##############################################################
par(mfrow=c(2,2),cex=0.75)

# a) Cooling phase
plot(cooleda$Time,cooleda$survmeano2sat,type="l",col="blue",lwd=2,
xlab="Time (in seconds)",ylab=expression(O[2]*" saturation(%)"),
main="a) Cooling phase",ylim=c(50,100))
lines(cooleda$Time,cooleda$nonsurvmeano2sat,col="red",lwd=2)
legend("topright",c("Survivors","Non-survivors"),
col=c("blue","red"),lwd=c(2,2))

# b) Hypothermia phase
plot(hypoeda$Time,hypoeda$survmeano2sat,type="l",col="blue",lwd=2,
xlab="Time (in seconds)",ylab=expression(O[2]*" saturation(%)"),
main="b) Hypothermia phase",ylim=c(50,100))
lines(hypoeda$Time,hypoeda$nonsurvmeano2sat,col="red",lwd=2)
```

```
legend("topright",c("Survivors","Non-survivors"),
col=c("blue","red"),lwd=c(2,2))

# c) Rewarming phase
plot(rewarmeda$Time,rewarmeda$survmeano2sat,type="l",col="blue",lwd=2,
xlab="Time(in seconds)",ylab=expression(O[2]*" saturation(%)"),
main="c) Rewarming phase",ylim=c(50,100))
lines(rewarmeda$Time,rewarmeda$nonsurvmeano2sat,col="red",lwd=2)
legend("topright",c("Survivors","Non-survivors"),
col=c("blue","red"),lwd=c(2,2))

# d) Normothermia phase
plot(normoeda$Time,normoeda$survmeano2sat,type="l",col="blue",lwd=2,
xlab="Time (in seconds)",ylab=expression(O[2]*" saturation(%)"),
main="d) Normothermia phase",ylim=c(50,100))
lines(normoeda$Time,normoeda$nonsurvmeano2sat,col="red",lwd=2)
legend("topright",c("Survivors","Non-survivors"),
col=c("blue","red"),lwd=c(2,2))

#####################################################################
#                        Variance Structure                         #
#####################################################################
par(mfrow=c(2,2))

# a) Cooling phase
par(mfrow=c(2,2), cex=0.75)
plot(cooleda$Time,cooleda$survvaro2sat,type="l",
col="blue",lwd=2,xlab="Time (in seconds)",
ylab="Variance",main="a) Cooling phase",ylim=c(0,160))
lines(cooleda$Time,cooleda$nonsurvvaro2sat,col="red",lwd=2)
legend("topright",c("Survivors","Non-survivors"),
col=c("blue","red"),lwd=c(2,2))

# b) Hypothermia phase
plot(hypoeda$Time,hypoeda$survvaro2sat,type="l",
col="blue",lwd=2,xlab="Time (in seconds)",
ylab="Variance",main="b) Hypothermia phase",ylim=c(0,160))
lines(hypoeda$Time,hypoeda$nonsurvvaro2sat,col="red",lwd=2)
legend("topright",c("Survivors","Non-survivors"),
col=c("blue","red"),lwd=c(2,2))

# c) Rewarming phase
plot(rewarmeda$Time,rewarmeda$survvaro2sat,type="l",
col="blue",lwd=2,xlab="Time (in seconds)",
ylab="Variance",main="c) Rewarming phase",ylim=c(0,160))
lines(rewarmeda$Time,rewarmeda$nonsurvvaro2sat,col="red", lwd=2)
legend("topright",c("Survivors","Non-survivors"),
```

```
col=c("blue","red"),lwd=c(2,2))

# d) Normothermia phase
plot(normoeda$Time,normoeda$survvaro2sat,type="l",
col="blue",lwd=2,xlab="Time (in seconds)",
ylab="Variance",main="d) Normothermia phase",ylim=c(0,160))
lines(normoeda$Time,normoeda$nonsurvvaro2sat,col="red",lwd=2)
legend("topright",c("Survivors","Non-survivors"),
col=c("blue","red"),lwd=c(2,2))

##############################################################
#                      Correlation Structure                 #
##############################################################

panel.cor<-function(x,y,digits=2,prefix="",cex.cor)
{
    usr<-par("usr");on.exit(par(usr))
    par(usr=c(0,1,0,1))
    r<-cor(x,y,use="complete.obs")
    txt<-format(c(r,0.123456789),digits=digits)[1]
    txt<-paste(prefix,txt,sep="")
    if(missing(cex.cor))cex<-1.0
    test<-cor.test(x,y)
    Signif<-symnum(test$p.value,corr=FALSE,na=FALSE,
                   cutpoints=c(0,0.05,1),
                   symbols=c("*"," "))
    text(0.5,0.5,txt,cex=cex)
    text(0.8,0.8,Signif,cex=cex,col=2)
}
pairs(~SctO2+oesophagale+rectal+CCO+CO2+pO2,
lower.panel=panel.smooth,upper.panel=panel.cor)

##############################################################
#                          Fitting GAMM                      #
##############################################################

# Model 1: Allowing curves to differ by patient group #
model1=gamm(SctO2~s(time,bs="cr")+s(time,by=as.numeric(Group==1)),
data=coolfin,random=list(patient=~1))

# Examine gam and lme parts of model
summary(model1$gam);summary(model1$lme)

# Plot the model terms#
plot(model1$gam,scale=0,xlab="Time (in minutes)",
ylab="f(Time)",main="c) Difference curve")
abline(a = 0, b = 0, col = "red",lty="dashed")
```

```
abline(v=42, col = "red",lty="dashed")
abline(v=73, col = "red",lty="dashed")
abline(v=165, col = "red",lty="dashed")
abline(v=225, col = "red",lty="dashed")

# Plot residuals versus time#
x1<-model1$lme;
plot(x1,resid(.,type="p")~time,main="d) Model diagnostic plot")

# Model 2: Without correction term
model2=gamm(SctO2~s(time,bs="cr"),data=coolfin,random=list(patient=~1))

# Examine gam and lme part of model
summary(model2$gam);summary(model2$lme)

# Plot the model terms
plot(model2$gam,scale=0,page=1)

# Plot residuals versus time
x2<-model2$lme;plot(x2,resid(.,type="p")~time)

# Model 3: Allowing constant group effect over time
model3=gamm(SctO2~Group+s(time,bs="cr"),data=coolfin,
random=list(patient=~1))

# Examine gam and lme part of model
summary(model3$gam);summary(model3$lme)

# Plot the model terms
plot(model3$gam,scale=0,page=1)

# Plot residuals versus time
x3<-model3$lme;plot(x3,resid(.,type="p")~time)

# Compute AIC values
AIC(model1$lme,model2$lme,model3$lme)
```

Auteursrechtelijke overeenkomst

Ik/wij verlenen het wereldwijde auteursrecht voor de ingediende eindverhandeling:
Effect of cooling post-cardiac arrest patients

Richting: **Master of Statistics-Biostatistics**
Jaar: **2011**

in alle mogelijke mediaformaten, - bestaande en in de toekomst te ontwikkelen - , aan de Universiteit Hasselt.

Niet tegenstaand deze toekenning van het auteursrecht aan de Universiteit Hasselt behoud ik als auteur het recht om de eindverhandeling, - in zijn geheel of gedeeltelijk -, vrij te reproduceren, (her)publiceren of distribueren zonder de toelating te moeten verkrijgen van de Universiteit Hasselt.

Ik bevestig dat de eindverhandeling mijn origineel werk is, en dat ik het recht heb om de rechten te verlenen die in deze overeenkomst worden beschreven. Ik verklaar tevens dat de eindverhandeling, naar mijn weten, het auteursrecht van anderen niet overtreedt.

Ik verklaar tevens dat ik voor het materiaal in de eindverhandeling dat beschermd wordt door het auteursrecht, de nodige toelatingen heb verkregen zodat ik deze ook aan de Universiteit Hasselt kan overdragen en dat dit duidelijk in de tekst en inhoud van de eindverhandeling werd genotificeerd.

Universiteit Hasselt zal mij als auteur(s) van de eindverhandeling identificeren en zal geen wijzigingen aanbrengen aan de eindverhandeling, uitgezonderd deze toegelaten door deze overeenkomst.

Voor akkoord,

Muthusi, Kimeu

Datum: **12/09/2011**